Local-Global Interaction on a Phase Space Based on Generative Pointer

Moto Kamiura[a,*], Kohei Nakajima[b] & Yukio-Pegio Gunji[c]

[a] Faculty of Science and Technology, Tokyo University of Science
[b] Graduate School of Arts and Sciences, The University of Tokyo
[c] Graduate School of Science / Faculty of Science, Kobe University

* kamiura@rs.noda.tus.ac.jp

Abstract Nonlinear dynamical systems show some different motions such as periodic, chaotic or intermittent ones. On-off intermittency is aperiodic switching motion between laminar phases and burst phases. It is observed in critical points with blowout bifurcation. Occurrence of it is sensitive with respect to parameter shifts in conventional systems. In the present paper, an extended dynamical system with an interaction between a global structure and a local motion is proposed. This interaction means a reciprocal definition between a parameter and state variables. The reciprocal definition is induced from the concept of a *generative pointer* that suggests an extended subobject classifier. Ubiquitous on-off intermittency is observed for a wide range of parameter values when a generative pointer is applied to a Henon map. This fact implies robustness of on-off intermittency against parameter shifts.

Keywords: Dynamical systems, Intermittency, Robustness, Emergence, Heterarchy.

1 Introduction

1.1 On-off intermittency based on criticality

Nonlinear dynamical systems show some different motions such as fixed point, periodic motion, chaos and intermittency. One has known some kinds of intermittency: e.g. Type I, II, III intermittency (Pomeau and Manneville 1980) and on-off intermittency (Platt et al. 1993; Heagy et al. 1994). On-off intermittency was discovered in a 2-dimensional coupled dynamical system (Fujisaka and Yamada 1985). It is aperiodic switching motion between laminar phases and burst phases. On the other hand, a high-dimensional chaotic system, which is called globally coupled map (GCM), has been also researched (Kaneko 1990). A GCM shows aperiodic switching between clustering and declustering, that is called chaotic itinerancy. Chaotic itinerancy provides a theoretical background of a model of stem cell differentiation (Furusawa and Kaneko 2001). The bursts of on-off intermittency and the declustering of chaotic itinerancy is based on destabilization of the invariant manifolds along the transverse to the manifolds. Such destabilization of the manifolds are induced from change of a parameter of these systems. The criticality on the parameter change is called blowout bifurcation (Ott and Sommerer 1994; Kanamaru 2006). I.e. on-off intermittency is closely related to chaotic itinerancy on the mechanism of the dynamical systems. On-off intermittency is a important research subject in complex systems science.

On-off intermittency occurs at critical points with nonhysteretic blowout bifurcation: i.e. it is fragile with respect to parameter shifts. This fact brings the following question: Doesn't such fragility contradict robustness of actual complex systems? Actual complex systems including biological systems seem to generate and to sustain appropriate complexity by themselves. What is the difference between the conventional dynamical systems and actual complex systems?

There can be an answer in the difference between hierarchy and heterarchy. Heterarchy is an extended hierarchy with dynamic interaction between the hierarchical layers (McCulloch 1945). Jen described heterarchy as the meta-structure carrying the robustness of systems (Jen 2003). Our studies have suggested that heterarchical structure enhances robustness of on-off intermittency in dynamical systems.

1.2 Heterarchy on dynamical systems

It is necessary to find hierarchical or heterarchical layers in a dynamical system as the first step. The mechanism of each dynamical system is characterized by the topology of the phase space (Rosen 1970). A continuous dynamical system is uniquely defined by a vector field. One can see that a vector field gives an invariant global structure and the 1-parameter transformation group induced from the vector field gives the local motion in a continuous dynamical system. i.e. there is hierarchical unidirectionality from a vector field to the 1-parameter transformation group. A discrete dynamical system is not defined by a vector field, but we can see a hierarchy also in a discrete dynamical system: one can construct a set of trajectories (i.e. a colimit of a category of a dynamical system) as a global structure of a dynamical system (Kamiura and Gunji 2006c). Moreover, a bifurcation diagram is constructed as a classification of trajectories on a parameter. A parameter indicates a sort of global layer of the system. On the other hand, state variables of a dynamical system belong to a local layer of the system. A parameter and state variables is found as a global layer and a local one, in both continuous system and discrete one. If hierarchical structure of a dynamical system is given by a parameter and state variables, then heterarchical one can be defined by interaction between a parameter layer and a variable layer.

Some heterarchical systems have already been researched: Gunji et al have studied the general formalization of the dynamic complementary relation using the framework of information theory (Gunji et al. 2003; 2006) and dynamical system theory (Kamiura and Gunji 2006b; 2006c). Moreover, using an extended Fujisaka-

Yamada (FY) system, they studied a coupled map system based on a heterarchical structure (i.e. Active Coupling System; ACS) (Gunji and Kamiura 2004; Kamiura and Gunij 2006a). An ACS consists of time evolutional maps derived from extended functors. Consequently, the transverse Lyapunov exponent of ACS is fluctuated near zero value by the time evolutional maps. As a result, on-off intermittency, which is a critical feature of the specific coupling parameter in FY system, occurs ubiquitously for all parameter values in ACS. This fact can be evaluated as the robustness of intermittency. This scheme has been applied to 1-dimensional logistic map. The map, also, shows on-off intermittency (Nakajima and Shinkai 2007).

In the present paper, one alternative to ACS is proposed to introduce heterarchy for a dynamical system. Indicating a singleton (or a state on phase space) is formalized by a *generative pointer*, which is an extended subobject classifier. A subobject classifier formalizes specifying a point or a subset. A generative pointer is applied to a phase space of a dynamical system. Consequently, dynamic change of the parameter of the system is induced. Being applied to a Henon map, a generative pointer is evaluated by the behavior of the map. We call the system the *extended Henon map based on Generative Pointers* (HGP) system.

1.3 Global layer depending on local layer

In the previous section, we saw that a local layer depends on a global layer in hierarchy. In contrast, it is not clear that the global layer depends on the local layer. In this section, such a dependence relation which is required for heterarchy is illustrated with emergence of rational numbers.

A multiplication, $n \times 3 = m (n \in \mathbb{N})$, can be expressed by the map $f_3 : \mathbb{N} \to \mathbb{N} : n \mapsto m = 3n$. If the division $m \div 3 = n$ is defined by $g_3 : \mathrm{Im}(f_3) \to \mathbb{N} : 3n \mapsto n$, then $g_3 = f_3^{-1}$. Therefore $g_3 \circ f_3 = id$ and $f_3 \circ g_3 = id$.

However, a new sign expressing "a fraction", such as 2/3, is required when the domain of the map g_3 is defined not by $\mathrm{Im}(f_3)$ but by $\mathbb{N}$. Moreover, we can regard the fractions as a following: i.e. the fractions such as 2/3 did not exist a priori, but they has been generated historically. Under this view, we can see the emergence of positive rational numbers $\mathbb{Q}^+$, when arbitrary natural numbers are substituted for the top and bottom blanks ($\square$) of the division sign "$\frac{\square}{\square}$".

One can express the map g_3 as the map $g_{3*} : \mathbb{N}_* \to \mathbb{N}_*$ on the pointed set $\mathbb{N}_* := \mathbb{N} \cup \{*\}$:

$$g_{3*}(x) = \begin{cases} g_3(x) & (\text{if } x \in \mathrm{Im}(f_3) = \{3n | n \in \mathbb{N}\} \subset \mathbb{N}) \\ * & (\text{if } x \in \mathbb{N}_* \backslash \mathrm{Im}(f_3) = \{3n+1 | n \in \mathbb{N}\} \cup \{3n+2 | n \in \mathbb{N}\}) \end{cases}$$

In this sense, by hiding or painting out the fractions by the point $*$, we can deal with only $\mathrm{Im}(f_3) = \{3n | n \in \mathbb{N}\}$ as the domain of g_3.

Now, we use the expressions such as "hide" or "paint out" since we know the concepts of division and rational numbers. However, if we focus on the emergence of fractions, we can suppose that the fractions are not hidden by the point $*$ but the concept of the region of the numbers is extended from natural numbers to rational numbers by replacing the sign "$*$" with the sign "$\frac{\square}{\square}$". In other words, the replacement of the point $*$ with the fraction sign "$\frac{\square}{\square}$" reveals the replacement of the operand $(*)$ with the operator $(\frac{\square}{\square})$. The point $*$ is an element on the pointed set $\mathbb{N}_*$ but "$\frac{\square}{\square}$" is a map in $\mathrm{Hom}(\mathbb{N} \times \mathbb{N}, \mathbb{Q}^+)$.

Needless to say, in an axiomatical theory, rational numbers are constructed as an equivalence class of ordered pairs of integers (a, b) with $b \neq 0$, and are induced by the equivalence relation $(a, b) \sim (c, d) \iff ad = bc$. Moreover, we do not insist that the above process on the signs is a historical fact. The above allegory only shows the following view: i.e. when local motion selects a point on the outside of range, a global structure can be changed, like the extention from natural numbers to rational numbers. In the following section, generative pointer is introduced as a model of such a view.

At the end of this section, we introduce a term, *Local Identity*, so as to use it in the following section.

Definition 1 (*Local Identity*) For topological spaces A and B such that the measure $M(A \cap B) \neq 0$ (i.e. $A \cap B$ is neither empty nor singleton), and for the subspace U such that $U \subset A \cap B$ and the measure $M(U) \neq 0$, if a map $Lid_U : A \to B$ is defined by

$$Lid_U(x) = \begin{cases} x & (\text{if } x \in U) \\ f(x) & (\text{if } x \in A \backslash U), \end{cases}$$

then we call the map Lid_U *local identity* on U, where $f : A \backslash U \to B$ is an arbitrary map. ■

Again, assume the multiplication map $f_3 : \mathbb{N} \to \mathbb{N}$. It naturally induces the map $f_{3*} : \mathbb{N}_* \to \mathbb{N}_*$ which is defined by $f_{3*}(x) = \begin{cases} f_3(x) & (\text{if } x \in \mathbb{N}) \\ * & (\text{if } x \in \{*\}) \end{cases}$. Composition of the maps $g_{3*} \circ f_{3*}$ and $f_{3*} \circ g_{3*}$ are local identities.

2 Generative pointer and application to a dynamical system

2.1 Characteristic function and subobject classifier

First, we consider a form of indication of a point (i.e. an element in a set). In set theory, separating a subset $B \subset A$ from the difference set $A \backslash B$ on a set A is formalized by a characteristic function. The characteristic function of a subset B is the two-valued function $m_B : A \to \{0, 1\}$ on A; $m_B(x) = \begin{cases} 0 & (\text{if } x \in B) \\ 1 & (\text{otherwise}) \end{cases}$. $\{0\} \subset \{0, 1\}$ represents the simplest non-trivial subset. An arbitrary subset $B \subset A$ can be mapped onto this simplest subset by m_B. This map produces a pullback square:

$$\begin{tikzcd} B \arrow[r] \arrow[d, tail, "p"'] & \{0\} \arrow[d, tail, "s"] \\ A \arrow[r, "m_B"] & \{0,1\}. \end{tikzcd} \tag{1}$$

One says that the monomorphism (the typical subset) s is a subobject classifier. If the subset A is a one-point set $\{a\}$, the subobject classifier corresponds to indicating the specific state a.

2.2 Pointer

Secondly, we modify the characteristic function to connect the indication of a point to the dynamic change of the domains and ranges.

Assume a conventional dynamical system $(D, \varphi(\beta))$. Given the state $x_t \in D$ at the time t, the system and the state induce the partial map $|\varphi(\beta)| : \{x_t\} \to \{x_{t+1}\} : x_t \mapsto x_{t+1}$, where the singleton $\{x_t\} = X_t$ $(t \in \mathbb{N})$ is a subspace of D. On the other hand, $\{x_t\}$ induces the natural monomorphism $p_t : \{x_t\} \to D : x_t \mapsto x_t$. Now, given a map $r : \{*\} \to I : * \mapsto r_0$, there is an isomorphism $m_t : D \to I$ such that the following diagram is a pullback:

$$\begin{tikzcd} X_t \arrow[r, "\iota"] \arrow[d, tail, "p_t"'] & \{*\} \arrow[d, tail, "r"] \\ D \arrow[r, "m_t"] & I \end{tikzcd} \qquad \begin{tikzcd} x_t \arrow[r, mapsto] \arrow[d, mapsto] & * \arrow[d, mapsto] \\ x_t \arrow[r, mapsto] & r_0 \end{tikzcd} \tag{2}$$

where I is a bounded open topological space. Now $I := (-1, 1)$ and r_0 is a random number in I. Note that the map m_t is not unique in the above case. In the diagram of the subobject classifier, I is defined in such a way as to uniquely determine m_t. However, in the above diagram (2), I is defined by $(-1, 1)$ first, and then m_t is chosen such that the diagram commutes.

We restrict the kind of the maps m_t to get back the uniqueness, i.e. we define the map by $m_t(a_t)(x_t) = \frac{2}{\pi} \arctan a_t x_t$, where a_t is a parameter and it is defined in such a way that the diagram (2) commutes, i.e. the uniqueness of the map m_t is replaced by that of the parameter a_t. Note that the above $m_t(a_t) : D \to I$ is a naturally isomorphic, continuous, smooth and odd function (i.e. preserving the positive and negative signs) if D is an open topological space $(-\infty, \infty)$. Since the $m_t(a_t)$ or m_t is defined as the isomorphism, there is an inverse map m_t^{-1}. Consequently, the inclusion p_t satisfies the composition $m_t^{-1} \circ r \circ \iota = p_t$. We call the map p_t with the above commutative diagram a *pointer*. In addition, in the pointer diagram defined above, if the map $r : \{*\} \to I : * \mapsto r_0$ is replaced by $r' : \{*\} \to I : * \mapsto r_1$, then a new pullback X'_t for r' and m_t is induced. This means that a new point $X'_t = \{x'_t\}$ on D is chosen by picking up the value r_1 on I. Since m_t is an isomorphism, we obtain $x'_t = m_t^{-1}(r_1) = \frac{1}{a_t}\tan\frac{\pi}{2}r_1$. By replacing r with r', the pointer p_t is replaced with p'_t, and, furthermore, x'_t (i.e. the outside of $\{x_t\}$) is chosen. The m_t governs the indication of the point on D.

2.3 Generative pointer

Thirdly, we introduce the map $m_t^\sharp : I \to D$ which is defined by $m_t^\sharp(r) := Dec[m_t^{-1}(r)]$, where $Dec[a]$ expresses the number of the decimal part of a real number a. In this definition, the map $m_t^\sharp$ has the image $\mathrm{Im}(m_t^\sharp) = I \subset D$. The maps m_t and $m_t^\sharp$ induce m_{t*} and $m_{t*}^\sharp$, which are morphisms on pointed sets. $m_{t*}^\sharp \circ m_{t*}$ and $m_{t*} \circ m_{t*}^\sharp$ are local identities as well as the compositions of the multiplication and the division, $g_{3*} \circ f_{3*}$ and $f_{3*} \circ g_{3*}$, in the previous section. The map $m_t^\sharp$ induces the following diagram:

$$\begin{tikzcd}
\widetilde{X}_t \arrow[r] \arrow[d, tail, "\widetilde{p}_t"'] & \{*\} \arrow[d, tail, "r'"] \\
D & I \arrow[l, "m_t^\sharp"]
\end{tikzcd}
\qquad\qquad
\begin{tikzcd}
\widetilde{x}_t \arrow[r, mapsto] \arrow[d, mapsto] & * \arrow[d, mapsto] \\
\widetilde{x}_t & r_1 \arrow[l, mapsto]
\end{tikzcd} \tag{3}$$

where $\widetilde{X}_t = \{\widetilde{x}_t\}$ is determined by $\widetilde{x}_t = m_t^\sharp(r_1)$, and the map $\widetilde{p}_t : \{\widetilde{x}_t\} \to D : \widetilde{x}_t \mapsto \widetilde{x}_t$ is a natural monomorphism. We call the map $\widetilde{p}_t$ with the above diagram a *generative pointer*.

2.4 Application to Henon map

Let us experiment with the generative pointer on a concrete dynamical system. Suppose a 2-dimensional dynamical system, $\Psi : D \times D \to D \times D : \langle x_t, y_t \rangle \mapsto \langle x_{t+1}, y_{t+1} \rangle$ where $D = (-\infty, \infty)$. Now we choose a Henon map for this system. Specifically, in a system with time evolution of the parameter β, it is expressed by

$$\begin{pmatrix} x_{t+1} \\ y_{t+1} \end{pmatrix} = \Psi \begin{pmatrix} x_t \\ y_t \end{pmatrix} = \begin{pmatrix} 1 - \alpha x_t^2 + \beta_t y_t \\ x_t \end{pmatrix}. \tag{4}$$

If β_t is a constant, then the above is a conventional Henon map. The above map induces a binary operation $\psi(\beta_t) : D \times D \to D : \langle x_t, y_t \rangle \mapsto x_{t+1}$, that is,

$$x_{t+1} := \psi(\beta_t)(x_t, y_t) = 1 - \alpha x_t^2 + \beta_t y_t \tag{5}$$

where β_t in $\psi(\beta_t)$ is explicitly expressed in a way that allows it to be emphasized as the parameter. Moreover, if the value of $y_t = x_{t-1}$ is fixed, an unary operation $\psi_{\beta_t, y_t} : D \to D : x_t \mapsto x_{t+1}$ is induced by the binary operation ψ_{β_t}.

Moreover, by the following procedure, time evolution of β_t is constructed.

[Step 1] Given a random number $r_t \in I = (-1, 1)$, the parameters a_t and a_{t+1} of m_t and m_{t+1} are set so as to satisfy the following equations: $m_t(x_t) = \frac{2}{\pi}\arctan a_t x_t = r_t$ and $m_{t+1}(x_{t+1}) = \frac{2}{\pi}\arctan a_{t+1} x_{t+1} = r_t$. I.e. a_t and a_{t+1} are given by $a_t = \frac{1}{x_t}\tan\frac{\pi}{2}r_t$ and $a_{t+1} = \frac{1}{x_{t+1}}\tan\frac{\pi}{2}r_t$.

[Step 2] For the above a_t, a_{t+1} and the random number $r'_t \in I\backslash\{r_t\}$, $\widetilde{x}_t$ and $\widetilde{x}_{t+1}$ are defined as $\widetilde{x}_t = m_t^\sharp(r'_t) = \frac{1}{a_t}\tan\frac{\pi}{2}r'_t$ and $\widetilde{x}_{t+1} = m_{t+1}^\sharp(r'_t) = \frac{1}{a_{t+1}}\tan\frac{\pi}{2}r'_t$. For these two values, $\widetilde{\beta}_t$ is chosen such that the following condition is satisfied:

$$\widetilde{x}_{t+1} = \psi_{\widetilde{\beta},\widetilde{y}_t}(\widetilde{x}_t) = 1 - \alpha\widetilde{x}_t^2 + \widetilde{\beta}_t\widetilde{y}_t \tag{6}$$

where $\widetilde{y}_t = \widetilde{x}_{t-1} = m_{t-1}^\sharp(r'_{t-1}) = \frac{1}{a_{t-1}}\tan\frac{\pi}{2}r'_{t-1}$ is the value given in the previous step in this calculation process. In other words, the previous recurrence equation (5) which gives a dynamical system is diverted to a definitional equation for β_t. Consiquently, under the condition that $\widetilde{y}_t \neq 0$, $\widetilde{\beta}_t$ is given by

$$\widetilde{\beta}_t := \frac{\widetilde{x}_{t+1} + \alpha\widetilde{x}_t^2 - 1}{\widetilde{y}_t}. \tag{7}$$

[Step 3] Using the above value of $\widetilde{\beta}_t$, β_{t+1} is defined by

$$\beta_{t+1} := \beta_0 + \delta\widetilde{\beta}_t \tag{8}$$

where the coefficient $\delta \ll \beta_0$ is a small constant. In the following numerical experiments, $\delta = 10^{-5}$. If $\{\widetilde{x}_{t+i}\}_{i\in\{-1,0,1\}} = \{x_{t+i}\}_{i\in\{-1,0,1\}}$, then $\widetilde{\beta}_t = \beta_0$, and hence $\beta_{t+1} = (1+\delta)\beta_0 \approx \beta_0$.

The parameter β_t and the state variables $\{x_t\}_{t\in\mathbb{Z}}$ of HGP reciprocally define each other. The above procedure is illustrated by the following diagrams:

$$\begin{tikzcd}
\text{[Step 1]} & x_t \arrow[rr, mapsto, "|\varphi(\beta_t)|"] \arrow[dr, "p_t \circ m_t"'] & & x_{t+1} \arrow[dl, "p_{t+1}\circ m_{t+1}"] & \Longrightarrow & \text{[Setp 2]} & \widetilde{x}_t \arrow[rr, mapsto, dashed, "\varphi(\widetilde{\beta}_t)"] & & \widetilde{x}_{t+1} \\
& & r_t & & & & & r'_t \arrow[ul, "m_t^\sharp"] \arrow[ur, "m_{t+1}^\sharp"'] & \\
\text{[Step 3]} & x_{t+1} \arrow[rr, mapsto, "\varphi(\beta_0+\widetilde{\beta}_t)"] & & x_{t+2} & \Longleftarrow & & & * \arrow[u, "r'"] &
\end{tikzcd} \tag{9}$$

3 Results

In this section, the numerical results are shown for the extended Henon map system defined in the previous section, which we call the HGP system. In all numerical experiments of the present paper, the coefficient of (8) is $\delta = 10^{-5}$.

As control experiments, we use a conventional Henon map and a Henon map with the parameter β with added Gaussian noises:

$$\begin{pmatrix} x_{t+1} \\ y_{t+1} \end{pmatrix} = \begin{pmatrix} 1 - \alpha x_t^2 + (\beta_0 + R_G)y_t \\ x_t \end{pmatrix} \tag{10}$$

where R_G is a Gaussian noise with a mean $\langle R_G \rangle = 0$ and a standard deviation $\sigma_{R_G} = 10^{-2}$.

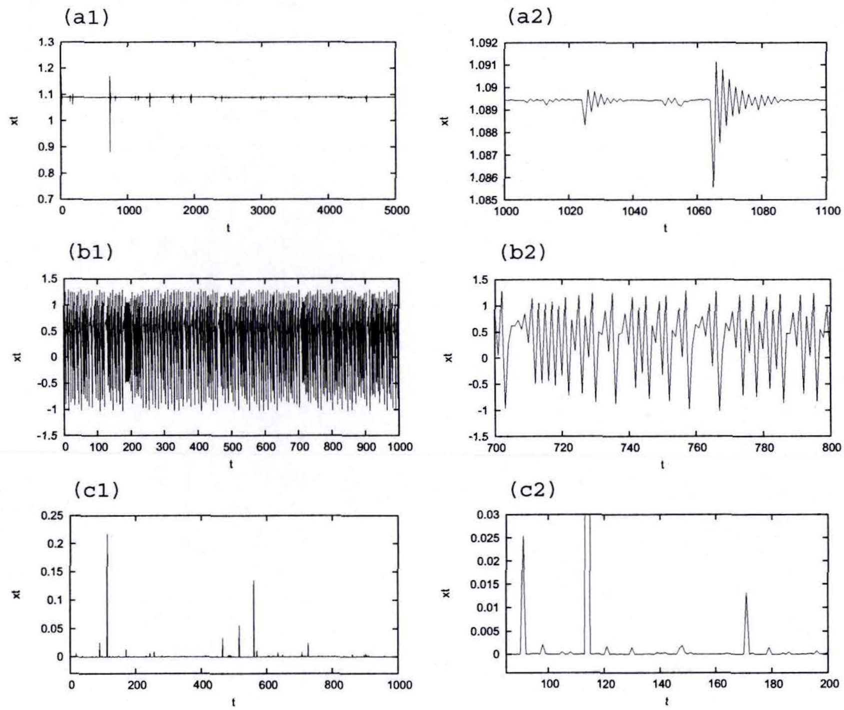

Fig. 1: (a1)-(b2) are the typical time series of x_t of the HGP: (a1) $\alpha = 0.2$, $\beta_0 = 0.3$ and $0 \leq t \leq 5000$. (a2) $\alpha = 0.2$, $\beta_0 = 0.3$ and $1000 \leq t \leq 1100$. (b1) $\alpha = 1.2$, $\beta_0 = 0.3$ and $0 \leq t \leq 1000$. (b2) $\alpha = 1.2$, $\beta_0 = 0.3$ and $700 \leq t \leq 800$. (c1)-(c2) are the typical time series of q_t derived from that of (b1): (c1) $\alpha = 1.2$, $\beta_0 = 0.3$ and $0 \leq t \leq 1000$. (c2) $\alpha = 1.2$, $\beta_0 = 0.3$ and $85 \leq t \leq 200$.

Fig.1 shows the typical time series of x_t of the HGP. A conventional Henon map shows a fixed point at $\alpha = 0.2$ and $\beta_0 = 0.3$. On the other hand, in HGP, on-off intermittency is observed instead for the same parameter values (Fig.1 (a1)-(a2)). Since intermittent motion is not clearly visible on x_t (Fig.1 (b1)-(b2)) for other values of α, we observe values of q_t that are defined by

$$q_t = |\psi(\beta_t)(x_t, y_t) - \psi(\beta_0)(x_t, y_t)| = |(\beta_t - \beta_0)y_t| = |\delta\widetilde{\beta}_t y_t|. \tag{11}$$

The values of q_t show on-off intermittency (Fig.1 (c1)-(c2)).

Fig.2 gives the bifurcation diagrams on (a) conventional Henon maps, (b) HGP and (c) Henon maps with Gaussian noises. Each diagram shows the values of x_t for

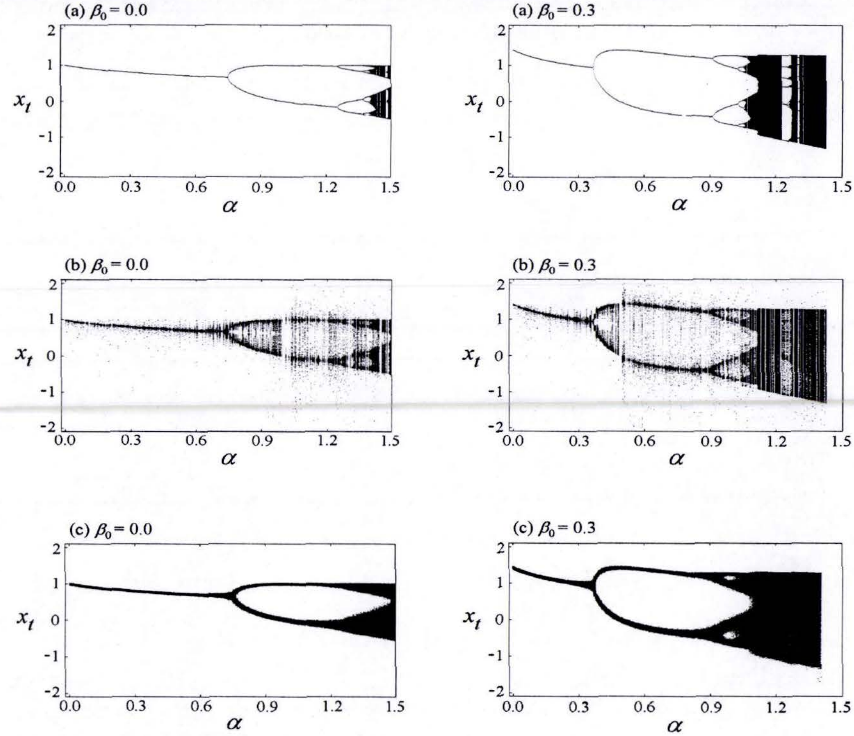

Fig. 2: The bifurcation diagrams on (a) conventional Henon maps, (b) HGPs and (c) Henon maps with Gaussian noises. Each diagram shows the values of x_t for $1000 \leq t \leq 4000$ along with the parameter $0.0 \leq \alpha \leq 1.5$. For the left and right figures, the initial parameter β_0 is given by $\beta_0 = 0.0$ and $\beta_0 = 0.3$ respectively.

$1000 \leq t \leq 4000$ along with the parameter $0.0 \leq \alpha \leq 1.5$. For the left and right figures, the initial parameter β_0 is $\beta_0 = 0.0$ and $\beta_0 = 0.3$, respectively. Conventionally, on-off intermittency is observed at critical points with blowout bifurcation, thus it is sensitive towards parameter shifts. Contrastingly, in the HGP, the on-off intermittency occurs within wide regions of α: within $0 < \alpha \lesssim 0.74$ for $\beta_0 = 0.0$ and within $0 < \alpha \lesssim 0.36$ for $\beta_0 = 0.3$ (Fig.2 (b)). The results show ubiquitous intermittency featuring robustness instead of stability. The irregular bursts of the intermittency form a bifurcation which is clearly different from the Gaussian noise with constant variance (Fig.2 (c)). This system with the Gaussian noise does not show the intermittency. Moreover, as will hereinafter be described in detail, in the time series of HGP, the value of x_t inevitably diverges after some time. If the divergence occurs sooner than 1000 steps in the time series, a blank region is formed on the bifurcation diagram. Consequently, the bifurcation diagrams of HGP have a window-like structure in the whole parameter region.

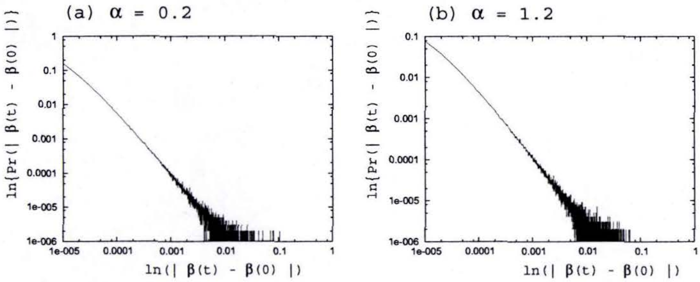

Fig. 3: The magnitude of fluctuation of β, $|\beta_t - \beta_0|$, versus the probability of that, $\Pr(|\beta_t - \beta_0|)$, on the HGP, where $\beta_0 = 0.3$ and (a) $\alpha = 0.2$ (b) $\alpha = 1.2$. Note that the graph is double logarithmic. These data consist of 100 trials, and each trial is observed until $t = 10^4$. The initial state (x_0, y_0) is chosen randomly for each trial. Each slope is (a) -1.83 and (b) -1.65.

Fig.3 shows the graphs of the magnitude of the fluctuation of β, $|\beta_t - \beta_0| = |\delta\widetilde{\beta}_t|$, versus the probability of that, $\Pr(|\beta_t - \beta_0|) = \Pr(|\delta\widetilde{\beta}_t|)$, on the HGP, where $\beta_0 = 0.3$ and (a) $\alpha = 0.2$ (b) $\alpha = 1.2$. Note that the graph is double logarithmic. Each slope is (a) -1.83 and (b) -1.65. These data consist of 100 trials and each trial is observed until $t = 10^4$. The initial state (x_0, y_0) is chosen at random for each trial. From the equation (11), we can know that the on-off intermittency of HGP is derived from $|\delta\widetilde{\beta}_t| \times |y_t|$ (i.e. the multiplication of the fluctuation of β and the state of HGP). In addition, $\Pr(|\delta\widetilde{\beta}_t|)$ follows a power law. As a result, we can see that $|\delta\widetilde{\beta}_t|$ scales up and down the state on the phase space.

In HGP, catastrophe (i.e. divergence of the value of x_t) inevitably occurs at some time. We call the time until the divergence occurs the *lifetime* of the system, T. Fig.4 shows the graph of the lifetime of HGP, T, versus the probability of that, $\Pr(T)$. In this case, the parameters of HGP are set to $\alpha = 0.2$ and $\beta_0 = 0.3$, and the divergence point is defined by the threshold $|x_t| > 10^5$. The data consist of 2×10^4 trials and each trial is observed until $t = 4 \times 10^4$. Note that the graph is single logarithmic, i.e. the graph is exponential and the system has a decay time constant $\tau \cong 8023$.

Why does such divergence occur? Fig.3 shows $\Pr(|\delta\widetilde{\beta}_t|) < 10^{-6}$ such that the fluctuation of β is $|\delta\widetilde{\beta}_t| > 0.1$, and hence big fluctuations occur rarely during the lifetime. If a fluctuation of ± 0.1 for β is attributed to the conventional Henon map, the Henon map has fixed points for $0.2 - 0.1 = 0.1 < \beta < 0.3 = 0.2 + 0.1$ and $\alpha = 0.3$, and the above divergence does not occur. Moreover, $m_t^\sharp$ is a bounded map on $(-1, 1)$, thus it is not the direct cause of the divergence. It is non-trivial that the

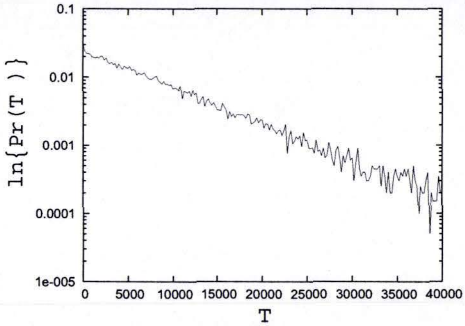

Fig. 4: The lifetime of HGP, T, versus the probability of that, $\Pr(T)$. The parameters of HGP are set to $\alpha = 0.2$ and $\beta_0 = 0.3$. The divergence point is defined by the threshold $|x_t| > 10^5$. The data consist of 2×10^4 trials, and each trial is observed until $t = 4 \times 10^4$. Note that the graph is single logarithmic, i.e. the graph is exponential and the system has a decay time constant $\tau \cong 8023$.

time series of the HGP diverge by about 8000 steps on the features of Henon maps and $m_t^\sharp$. The divergence of the time series may be derived from the conglomerate of the Henon map and the generative pointer. The analysis of statistics and the structure of the system remains the future works.

4 Conclusion

In the present paper, we introduced the concept of generative pointer, which are an extended subobject classifier with local identity. The generative pointer is introduced as the model of points being selected on the outside of the ranges.

In a conventional dynamical system, when a state is given on a phase space, the state has time evolution that is consistent with the global structure of the phase space. One can say that such an unidirectional dependency is hierarchical. In contrast, in HGP, the parameter and the state variables are reciprocally defined. I.e. the global structure is virtual and temporal, since the equation is locally constructed. Dynamic changes in the global structure are induced from indicating the local state by the generative pointer. Each step of the time evolution is defined on the temporal phase spaces. HGP has a heterarchical dependency between the global structure and the local motion.

In a conventional system, on-off intermittency is observed at critical points with blowout bifurcation. Therefore it is sensitive with respect to parameter shifts. On the contrary, in HGP, the on-off intermittency occurs for the wide range of the parameter valuesas, as well as ACS. The result shows the ubiquitous intermittency featuring robustness instead of stability.

Acknowledgment

This research was supported by the Sasagawa Scientific Research Grant from The Japan Science Society. We are grateful to Dr. Taichi Haruna (Kobe University) for technical guidance.

References

[1] Fujisaka,H. and Yamada,T. (1985) Prog. Theor. Phys. **74**, 918-921.

[2] Grebogi,C., Ott,E. and Yorke,J.A. (1982) Phys.Re,.Lett. **48**, 1507-1510.

[3] Gunji,Y-P., Ito,K. and Kusunoki,Y. (1997) Physica D **110**, 289-312.

[4] Gunji,Y.-P., Takahasi,T and Kamiura,M. (2003) Int. J. of Computing Anticipatory Systems **14**, 172-184.

[5] Gunji,Y.-P. and Kamiura,M. (2004) Physica D **198**, 74-105.

[6] Gunji,Y.-P., Miyoshi,H., Takahashi,T and Kamiura,M. (2006) Chaos, Solitons Fractals, **27**, 1187-1204.

[7] Heagy,J.F., Platt,N., and Hammel,S.M. (1994) Phys.Rev.E **49**, 1140-1150.

[8] Jen,E. (2005) Complexity **8**, 12-18.

[9] Kamiura,M. and Gunji,Y.-P. (2006a) Physica D **218**, 122-130.

[10] Kamiura,M. and Gunji,Y.-P. (2006b) Proc. of 6th Int. Workshop on Emergent Synthesis, 165-171.

[11] Kamiura,M. and Gunji,Y.-P. (2006c) Int. J. of Computing Anticipatory Systems **17**, 47-60.

[12] Kanamaru, T. (2006) Int. J. Bifurcation and Chaos **11**, 3309-3321.

[13] McCulloch,W.S. (1945) Bull.Math.Biophys. **7**, 89-93.

[14] Nakajima,K. and Shinkai,S. (2007) The conference proceedings of BIOCOMP2007, 301-308.

[15] Ott, E and Sommerer,J.C. (1994) Phys. Lett. A **188**, 39-47.

[16] Platt,N., Spiegel,E.A. and Tresser,C. (1993) Phys.Rev.Lett. **70**, 279-282.

[17] Pomeau,Y. and Manneville,P. (1980) Commun.Math.Phys. **74**, 189-197.

[18] Rosen,R. (1970) *Dynamical System Theory in Biology*, John Wiley Sons, New York.